



Cite this: RSC Adv., 2018, 8, 29495

Received 28th June 2018  
 Accepted 5th August 2018  
 DOI: 10.1039/c8ra05533e  
[rsc.li/rsc-advances](http://rsc.li/rsc-advances)

## Novel encapsulation of water soluble inorganic or organic ingredients in melamine formaldehyde microcapsules to achieve their sustained release in an aqueous environment†

Cong Sui, <sup>ab</sup> Jon A. Preece, <sup>c</sup> Shu-Hong Yu <sup>b</sup> and Zhibing Zhang <sup>\*a</sup>

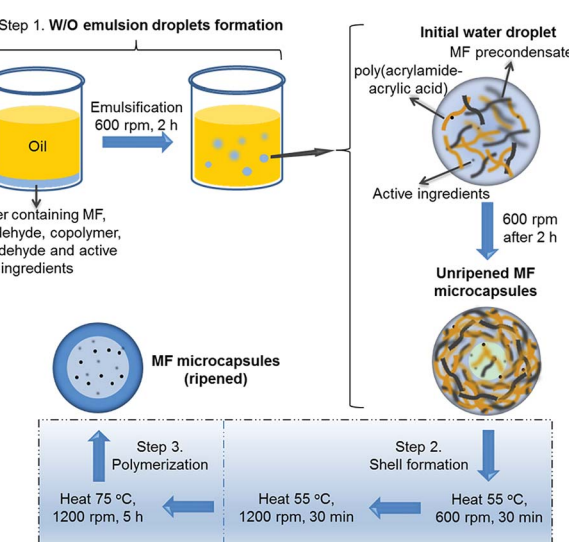
A novel type of melamine formaldehyde microcapsule with a desirable barrier has been used to encapsulate water soluble ingredients, including potassium chloride (KCl) and allura red (dye) as models of an inorganic salt and organic molecule, respectively, *via* a facile method, and it has shown a sustained release of KCl and allura red for 12 h and 10 days in aqueous environment, respectively.

Microencapsulation is an important technology to stabilise active ingredients and/or control their release for a range of industrial sectors including healthcare, household care, cosmetics and agrochemicals.<sup>1–3</sup> Various techniques including interfacial polymerisation, *in situ* polymerisation, solvent evaporation and coacervation, have been developed to encapsulate different types of active ingredients, such as oil-soluble, water-soluble, amphiphilic, powders or cells.<sup>4–8</sup> Encapsulation of water-soluble active ingredients is usually achieved by forming a water in oil (W/O) emulsion, initially stabilised by the self-assembly of molecular and/or polymolecular surfactants at the liquid/liquid interface, followed by further consolidation through chemical cross-linking of the surfactants at the interface, leading to robust isolatable capsules.<sup>2,9</sup> The actives that have been encapsulated range from biomacromolecules, such as proteins,<sup>3</sup> polysaccharides,<sup>10</sup> and enzymes<sup>11,12</sup> to small molecules, such as doxorubicin,<sup>10,13</sup> peroxide,<sup>14</sup> polyphenols,<sup>15</sup> and inorganic salts.<sup>16,17</sup>

Melamine formaldehyde (MF) is a versatile chemical cross-linking agent and has been broadly used in a number of encapsulation applications, due to its polycondensates providing a tight seal, thermal and mechanical stability and acid/alkaline resistance.<sup>18–20</sup> MF polycondensates have been used as shell material to encapsulate oils in applications in the area of carbonless copy paper,<sup>21</sup> fragrant oil<sup>22,23</sup> and herbicide/

insecticide delivery.<sup>24</sup> However, it has not been possible to form microcapsules, which can encapsulate water soluble ingredients and achieve a sustained release. Herein, we have developed a novel way to synthesise MF microcapsules *via* an *in situ* polymerisation process (Scheme 1) with a water soluble inorganic salt (KCl) and an organic dye (allura red), which displayed prolonged release times of 12 h and 10 days, respectively.

An aqueous phase containing the MF precondensate solution, formaldehyde, poly(acrylamide-acrylic acid) copolymer and the active (KCl or allura red) with the pH adjusted to 4.3, was emulsified within an oil (sunflower oil) phase at a stirring speed of 600 rpm (Scheme 1, Step 1) to form a Pickering emulsion (unripened (low-level cross-linking) microcapsules), with the MF and copolymer acting as the stabilising surfactants



Scheme 1 Illustration of MF microcapsules synthesised *via* an *in situ* polymerisation process with water soluble ingredients (KCl salt/allura red molecules) encapsulated.

<sup>a</sup>School of Chemical Engineering, University of Birmingham, UK. E-mail: Z.Zhang@bham.ac.uk

<sup>b</sup>Division of Nanomaterials & Chemistry, Hefei National Laboratory for Physical Sciences at the Microscale, Collaborative Innovation of Suzhou Nano Science and Technology, Department of Chemistry, CAS Centre for Excellence in Nanoscience, Hefei Science Centre of CAS, University of Science and Technology of China, Hefei 230026, China

<sup>c</sup>School of Chemistry, University of Birmingham, Edgbaston, Birmingham B15 2TT, UK

† Electronic supplementary information (ESI) available: Experimental section. See DOI: 10.1039/c8ra05533e

at the liquid/liquid interface.<sup>25,26</sup> The unripened MF microcapsules were then heated at 55 °C at 600 rpm for 30 min, which partially solidified the outer shell,<sup>27</sup> and the stirring speed was then increased to 1200 rpm, which was maintained for a further 30 min, to prevent aggregation between the unripened microcapsules (Step 2). The fully ripened MF microcapsules were finally formed by heating at 75 °C at 1200 rpm for a further 5 h (Step 3). The MF-KCl microcapsules (ripened) formed with different volumes of formaldehyde solution (200 µl and 600 µl, 37% (aq.) w/w) were named as MF-KCl (200 F) and MF-KCl (600 F), respectively.

The W/O emulsion droplets were stabilised by the pre-cross-linked MF precondensate and copolymer at pH 4.3, which adsorbed at the interface of the emulsion as shown in the optical micrograph (Fig. 1a), forming the unripened MF microcapsules with a core–shell structure. After preheated at 55 °C for 30 min, the unripened MF microcapsules partly solidified and they were strong enough to survive when the stirring speed increased to 1200 rpm, to avoid aggregation between microcapsules (Fig. S1†). The unripened microcapsules maintained their shapes and sizes after the stirring speed was increased as shown in Fig. S1b.† The formed ripened MF-KCl and MF-dye microcapsules showed spherical shapes on the microscale, and the MF-dye revealed a red core under the optical microscope, indicating the encapsulated dye in the MF microcapsules (Fig. 1b and c). The MF-KCl (600 F) revealed a smoother surface than the MF-KCl (200 F) one, which resulted from the increasing amount of formaldehyde integrated into

the MF polymerisation process (Fig. 1d and e). The size distributions exhibited in Fig. 1f show similar mean size [ $D(4,3)$ ] which were around 13 µm (Table 1). Clearly, the mean size varied with the viscosity of the prepared aqueous solution, and it slightly decreased with the decreasing viscosity of solution. The three batches of MF samples thus showed similar size distributions.

The cross-sections of MF-KCl (200 F) and MF-KCl (600 F) microcapsules are shown in Fig. 2, indicating clear shell structures. The MF-KCl (200 F) microcapsules displayed a thicker shell (0.65 (±0.04) µm to 1.30 (±0.09) µm) with a uniformly distributed core than MF-KCl (600 F) microcapsules (0.59 (±0.03) µm to 1.09 (±0.05) µm) with an inhomogeneously distributed core. The high concentration of formaldehyde in MF-KCl (600 F) led to the excess amount of formaldehyde in the water phase and might increase the polymerisation rate between MF precondensate and free formaldehyde, forming the unevenly distributed self-assembled solid MF core. Meanwhile, it led to higher local concentrations of formaldehyde, forming a smoother and more compact surface (Fig. 1e). The shell thicknesses of MF-KCl (600 F) microcapsules were thus thinner than those of MF-KCl (200 F) microcapsules due to the less amount of MF assembled in the shell. The elemental compositions of shell and core of MF-KCl (200 F) microcapsules confirmed by the energy dispersive X-ray (EDX) analysis, demonstrate that both of the shell and core contained C, N, Na and Cl, revealing the existing of assembled MF precondensate and copolymer (Fig. S2†). Meanwhile, the detectable K element in the core indicates that the K<sup>+</sup> ions were encapsulated in the MF microcapsules. The formed MF microcapsules were characterised by the Fourier-transform infrared (FT-IR) spectrometry. The absorption peaks of N–H stretching vibration at around 3340, 1559 and 813 cm<sup>−1</sup>, the C–N stretching at around 1358 cm<sup>−1</sup>, the C–H stretching at around 2938 and 1180 cm<sup>−1</sup>

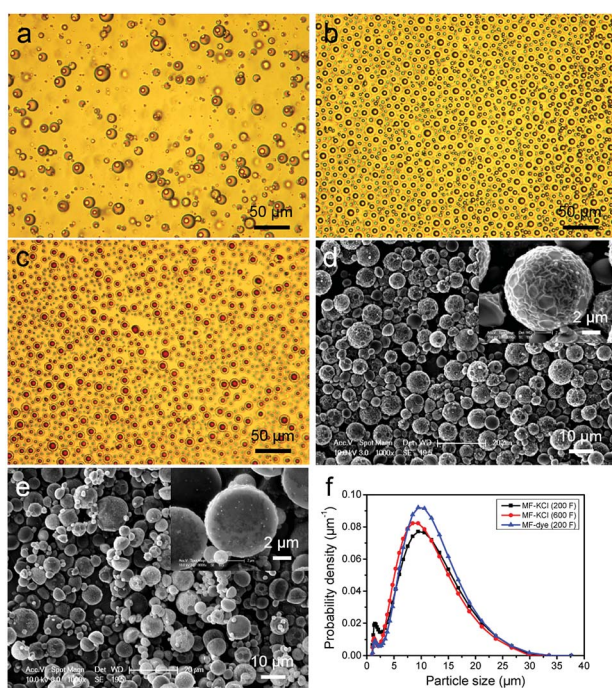


Fig. 1 Optical micrographs of (a) unripened MF-KCl (200 F) microcapsules produced at 600 rpm for 2 h, (b) MF-KCl (200 F) microcapsules and (c) MF-dye (200 F) microcapsules dispersed in water. SEM images of (d) MF-KCl (200 F) and (e) MF-KCl (600 F) microcapsules, and (f) the size distributions of MF-KCl (200 F), MF-KCl (600 F) and (e) MF-dye (200 F) microcapsules.

Table 1 The SPAN and mean size [ $D(4,3)$ ] of size distributions and viscosity data of initially mixed aqueous solution (before emulsification) for each batch of MF samples. The figure after ± represents the standard error of the mean

Sample	Mean size [ $D(4,3)$ ] (µm)	SPAN	Viscosity (Pa s)
MF-KCl (200 F)	13 (±1)	1.26 (±0.01)	0.0187 (±7 × 10 <sup>−4</sup> )
MF-KCl (600 F)	12 (±1)	1.26 (±0.02)	0.0169 (±7 × 10 <sup>−4</sup> )
MF-dye (200 F)	13 (±1)	1.21 (±0.05)	0.0188 (±8 × 10 <sup>−4</sup> )

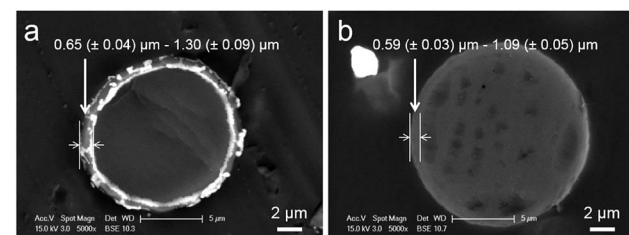


Fig. 2 TEM images of the cross-section of (a) MF-KCl (200 F) and (b) MF-KCl (600 F) microcapsules embedded in epon/araldite resin. (Each data was calculated from at least 30 microcapsules).

and the methylol at roughly  $1010\text{ cm}^{-1}$ , are the characteristics of MF and copolymer.<sup>28–30</sup> The slight shift of carboxyl group at  $1671\text{ cm}^{-1}$  for MF-KCl, might be due to the interactions between the carboxyl groups of copolymer and  $\text{K}^+$  ions, relative to the peak at  $1663\text{ cm}^{-1}$  for the neat MF as shown in Fig. S3.<sup>†</sup>

The microcapsules were dispersed in water and the release of  $\text{K}^+$  ions or dye molecules from the microcapsules were monitored, *via* removal of aliquots at extended time intervals over 12 hours and 10 days, and analysis with flame photometry ( $\text{K}^+$ ) and UV/Vis spectroscopy (dye), respectively. The cumulative release data of  $\text{K}^+$  ions in Fig. 3a from two batches of MF-KCl microcapsules demonstrates a sustained release within 2 hours, reaching roughly 90% of the encapsulated ions released out, and then followed by a slow release up to 12 h, which might be due to the interaction between  $\text{K}^+$  and carboxyl groups of copolymer as indicated by FT-IR (Fig. S3<sup>†</sup>). Interestingly, the release of  $\text{K}^+$  ions from MF-KCl (600 F) with more content of formaldehyde revealed a slower release rate, which may be attributed to the formed more compact MF, providing a barrier to the encapsulated ions, compared to MF-KCl (200 F). The release rate of allura red (dye) molecules from MF (200 F) displayed a sustained release, revealing a fast release leaking  $36 \pm 1\%$  within 2 h and then slowed down, leaking  $56.8 \pm 0.4\%$  for 10 days (Fig. 3b). The chemical structure of the released allura red (dye) molecules was not checked, since it had been demonstrated to be stable in acidic pH and at temperatures up to  $80\text{ }^\circ\text{C}$ .<sup>32</sup> The payloads and encapsulation efficiencies of KCl and dye in the MF microcapsules were calculated using the equations in Experimental section of the ESI<sup>†</sup> as shown in Table 2. Clearly, the ones for dye in MF microcapsules were higher than for KCl ions, which probably resulted from the larger molar mass of allura red, and its functional groups (Fig. S4<sup>†</sup>) might interact with MF and the copolymer. Regarding encapsulation of small water soluble ingredients, the commonly used liposomes also exhibited their sustained release for  $<24\text{ h}$  in water,<sup>33,34</sup> but the obvious drawbacks

are the fast release of the ingredients, high cost, low payload, low reproducibility and instability during storage.<sup>35</sup> In contrast, the MF microcapsules fabricated here are cheap and reproducible, and they display stable structure for 2 months in ethanol (Fig. S5<sup>†</sup>).

The mechanical properties of MF microcapsules were measured by a micromanipulation technique.<sup>36</sup> A single MF microcapsule was compressed by two parallel flat surfaces (Fig. 4a and b), and a force *versus* displacement curve for compression of the single MF-KCl (200 F) microcapsule was obtained as shown in Fig. S6.<sup>†</sup> The relationship of force ( $F$ ) *versus* displacement ( $\delta$ ) is assumed to represent the elastic behavior, when the nominal deformation calculated by eqn (1) is  $\leq 10\%$ , described by the Hertz model as given in eqn (2).<sup>37</sup>  $d$  is the diameter of the microcapsule;  $E$  is the Young's modulus of the microcapsules and  $\nu$  is the Poisson's ratio.

$$\text{Nominal deformation}(\%) = \frac{\delta}{d} \times 100 \quad (1)$$

$$F = \frac{4}{3} \frac{E}{(1 - \nu^2)} R^{1/2} \left( \frac{\delta}{2} \right)^{3/2} \quad (2)$$

In this way, a force *vs.*  $(\delta/2)^{3/2}$  curve was fitted with the Hertz model [eqn (2)], see Fig. 4c, and they are in good agreements with a correlation coefficient of 0.99, which justifies the assumption of the elastic behavior when the nominal deformation is  $\leq 10\%$ . The Young's modulus values of the three batches of MF microcapsules are showed in Table 2, and the MF-KCl (200 F) microcapsules formed with the less amount of formaldehyde indicates a higher Young's value due to the thicker shells and uniform cores, relative to the MF-KCl (600 F) microcapsules with an interstitial hollow core. In general, the Young's modulus of the formed MF microcapsules with a range of 2.8–4.9 GPa displayed a similar value, relative to previous researches, and the larger shell thickness could enhance the stiffness of the microcapsule.<sup>38,39</sup>

In conclusion, a novel method to synthesise MF microcapsules with aqueous phase encapsulated was developed in this study, and the water soluble ingredients, including an ion ( $\text{K}^+$ ) and small molecule (allura red) were encapsulated, indicating a sustained release in water environment for 12 h and 10 days, respectively. In addition, the formed MF microcapsules displayed Young's modulus values in the order of GPa, revealing comparatively strong stiffness. Therefore, the developed MF formation method may provide a new way to deliver different kinds of water soluble ingredients except those sensitive to acidic pH, which can have applications in different areas of scientific research and industry.

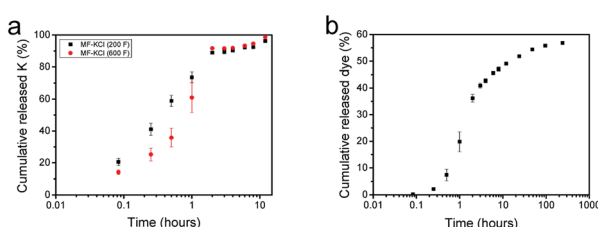


Fig. 3 Cumulative release profiles of (a)  $\text{K}^+$  ions from MF-KCl (200 F) microcapsules, MF-KCl (600 F) microcapsules and (b) dye molecules from MF-dye (200 F) microcapsules dispersed in water at  $37\text{ }^\circ\text{C}$  with shaking at a speed of 150 rpm. (Each experiment was conducted at least 3 times).

Table 2 The F/M (molar ratio), payload, encapsulation efficiency and Young's modulus of each batch of MF samples

Sample	F/M molar ratio	Payload (%)	Encapsulation efficiency (%)	Young's modulus (GPa)
MF-KCl (200 F)	0.7	$7.7 (\pm 0.3)$	$70 (\pm 2)$	$3.3 (\pm 0.2)$
MF-KCl (600 F)	1.7	$7.2 (\pm 0.1)$	$69 (\pm 2)$	$2.8 (\pm 0.2)$
MF-dye (200 F)	0.7	$8.4 (\pm 0.1)$	$82 (\pm 1)$	$4.9 (\pm 0.2)$



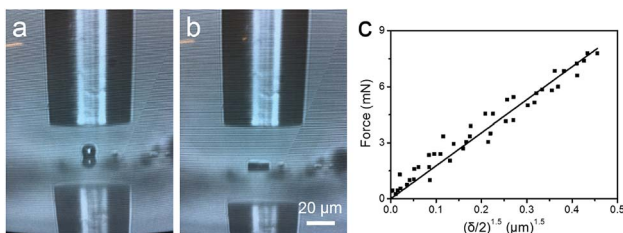


Fig. 4 Optical images obtained from screen (a) before and (b) after compressing a single MF microcapsule to large deformation. (c) The linear fit of the Hertz model to the data from compression of a single MF-KCl (200 F) microcapsule to 10% nominal deformation of its diameter. The compression speed was  $2 \mu\text{m s}^{-1}$ .

## Conflicts of interest

There are no conflicts to declare.

## Acknowledgements

C. S. was fully sponsored by College of Engineering & Physical Sciences, the University of Birmingham, UK.

## Notes and references

- 1 R. Ciriminna and M. Pagliaro, *Chem. Soc. Rev.*, 2013, **42**, 9243–9250.
- 2 R. Ciriminna, M. Sciortino, G. Alonzo, A. de Schrijver and M. Pagliaro, *Chem. Rev.*, 2011, **111**, 765–789.
- 3 S. Mitragotri, P. A. Burke and R. Langer, *Nat. Rev. Drug Discovery*, 2014, **13**, 655–672.
- 4 F. Casanova and L. Santos, *J. Microencapsulation*, 2016, **33**, 1–17.
- 5 N. V. N. Jyothi, P. M. Prasanna, S. N. Sakarkar, K. S. Prabha, P. S. Ramaiah and G. Y. Srawan, *J. Microencapsulation*, 2010, **27**, 187–197.
- 6 B. J. Kim, T. Park, H. C. Moon, S. Y. Park, D. Hong, E. H. Ko, J. Y. Kim, J. W. Hong, S. W. Han, Y. G. Kim and I. S. Choi, *Angew. Chem., Int. Ed.*, 2014, **53**, 14443–14446.
- 7 H. Lee, C. H. Choi, A. Abbaspourrad, C. Wesner, M. Caggioni, T. Zhu and D. A. Weitz, *ACS Appl. Mater. Interfaces*, 2016, **8**, 4007–4013.
- 8 M. Windbergs, Y. Zhao, J. Heyman and D. A. Weitz, *J. Am. Chem. Soc.*, 2013, **135**, 7933–7937.
- 9 J. Zhang, R. J. Coulston, S. T. Jones, J. Geng, O. A. Scherman and C. Abell, *Science*, 2012, **335**, 690–694.
- 10 C. Sui, Y. Lu, H. L. Gao, L. Dong, Y. Zhao, L. Ouali, D. Benczedi, H. Jerri and S. H. Yu, *Cryst. Growth Des.*, 2013, **13**, 3201–3207.
- 11 M. J. Abdekhodaie, J. Cheng and X. Y. Wu, *Chem. Eng. Sci.*, 2015, **125**, 4–12.
- 12 P. H. R. Keen, N. K. H. Slater and A. F. Routh, *Langmuir*, 2014, **30**, 1939–1948.
- 13 Y. Zhao, Z. Luo, M. H. Li, Q. Y. Qu, X. Ma, S. H. Yu and Y. L. Zhao, *Angew. Chem., Int. Ed.*, 2015, **54**, 919–922.
- 14 E. M. Dogan, F. Sudur Zalluhoglu and N. Orbey, *AIChE J.*, 2017, **63**, 409–417.
- 15 A. Elabbadi, N. Jeckelmann, O. P. Haefliger and L. Ouali, *J. Microencapsulation*, 2011, **28**, 1–9.
- 16 J. Bhaumik, N. S. Thakur, P. K. Aili, A. Ghanghoriya, A. K. Mittal and U. C. Banerjee, *ACS Biomater. Sci. Eng.*, 2015, **1**, 382–392.
- 17 C. Sui, J. A. Preece and Z. Zhang, *RSC Adv.*, 2017, **7**, 478–481.
- 18 D. Chen, H. Zhu, S. Yang, N. Li, Q. Xu, H. Li, J. He and J. Lu, *Adv. Mater.*, 2016, **28**, 10443–10458.
- 19 J. Ge, H. Y. Zhao, H. W. Zhu, J. Huang, L. A. Shi and S. H. Yu, *Adv. Mater.*, 2016, **28**, 10459–10490.
- 20 C. P. Ruan, K. L. Ai, X. B. Li and L. H. Lu, *Angew. Chem., Int. Ed.*, 2014, **53**, 5556–5560.
- 21 M. A. White, *J. Chem. Educ.*, 1998, **75**, 1119.
- 22 A. Ghaemi, A. Philipp, A. Bauer, K. Last, A. Fery and S. Gekle, *Chem. Eng. Sci.*, 2016, **142**, 236–243.
- 23 R. Mercade-Prieto, R. Allen, Z. B. Zhang, D. York, J. A. Preece and T. E. Goodwin, *AIChE J.*, 2012, **58**, 2674–2681.
- 24 M. Pretzl, M. Neubauer, M. Tekaat, C. Kunert, C. Kuttner, G. Leon, D. Berthier, P. Erni, L. Ouali and A. Fery, *ACS Appl. Mater. Interfaces*, 2012, **4**, 2940–2948.
- 25 A. Schrade, K. Landfester and U. Ziener, *Chem. Soc. Rev.*, 2013, **42**, 6823–6839.
- 26 Y. Long, B. Vincent, D. York, Z. B. Zhang and J. A. Preece, *Chem. Commun.*, 2010, **46**, 1718–1720.
- 27 D. J. Merline, S. Vukusic and A. A. Abdala, *Polym. J.*, 2013, **45**, 413.
- 28 X. D. He, X. W. W. Ge, M. Z. Wang and Z. C. Zhang, *Polymer*, 2005, **46**, 7598–7604.
- 29 K. Hong and S. Park, *Mater. Chem. Phys.*, 1999, **58**, 128–131.
- 30 N. Seetapan, N. Limpanyoon and S. Kiatkamjornwong, *Polym. Degrad. Stab.*, 2011, **96**, 1927–1933.
- 31 P. Lanthong, R. Nuisin and S. Kiatkamjornwong, *Carbohydr. Polym.*, 2006, **66**, 229–245.
- 32 K. Rovina, S. Siddiquee and S. M. Shaarani, *Front Microbiol.*, 2016, **7**, 798.
- 33 J.-Y. Fang, W.-R. Lee, S.-C. Shen and Y.-L. Huang, *J. Dermatol. Sci.*, 2006, **42**, 101–109.
- 34 Q. Lu, D.-C. Li and J.-G. Jiang, *J. Agric. Food Chem.*, 2011, **59**, 13004–13011.
- 35 A. Munin and F. Edwards-Lévy, *Pharmaceutics*, 2011, **3**, 793–829.
- 36 Z. Zhang, R. Saunders and C. R. Thomas, *J. Microencapsulation*, 1999, **16**, 117–124.
- 37 J. Hu, H.-Q. Chen and Z. Zhang, *Mater. Chem. Phys.*, 2009, **118**, 63–70.
- 38 J. F. Su, J. Qiu, E. Schlangen and Y. Y. Wang, *Constr. Build. Mater.*, 2015, **74**, 83–92.
- 39 R. Mercade-Prieto, R. Allen, D. York, J. A. Preece, T. E. Goodwin and Z. B. Zhang, *Chem. Eng. Sci.*, 2011, **66**, 1835–1843.

